QUANTITATIVE FINANCE
RESEARCH CENTRE

UNIVERSITY OF
TECHNOLOGY SYDNEY


THINK.CHANGE.DO

# QUANTITATIVE FINANCE RESEARCH CENTRE

Research Paper 264 December 2009

# Simulation of Diversified Portfolios in a Continuous Financial Market

Eckhard Platen and Renata Rendek

ISSN 1441-8010 www.qfrc.uts.edu.au

# Simulation of

# Diversified Portfolios in a Continuous Financial Market

**Eckhard Platen** [1] and **Renata Rendek**[1]

December 1, 2009

**Abstract.** In this paper we analyze the simulated behavior of diversified portfolios in a continuous financial market. In particular, we focus on equally weighted portfolios. We illustrate that these well diversified portfolios constitute good proxies of the growth optimal portfolio. The multi-asset market models considered include the Black-Scholes model, the Heston model, the ARCH diffusion model, the geometric Ornstein-Uhlenbeck volatility model and the multi-currency minimal market model. The choice of these models was motivated by the fact that they can be simulated almost exactly and, therefore, very accurately also over longer periods of time. Finally, we provide examples, which demonstrate the robustness of the diversification phenomenon when approximating the growth optimal portfolio of a market by an equal value weighted portfolio. Significant outperformance of the market capitalization weighted portfolio by the equal value weighted portfolio can be observed for models.

2000 *Mathematics Subject Classification:* 91B28, 62P05, 62P20

*Key words and phrases:* Growth optimal portfolio, Diversification Theorem, diversified portfolios, equally weighted portfolio, exact simulation.

[1]University of Technology Sydney, School of Finance & Economics and Department of Mathematical Sciences, PO Box 123, Broadway, NSW, 2007, Australia

# 1 Introduction

Diversification is a concept that has been successfully applied for centuries. When constructing a *diversified portfolio* (DP) the proportion of the value of the holding in any individual security, relative to the total portfolio value, converges sufficiently fast to zero as the number of securities increases. In the literature related to portfolio optimization DPs play a significant role, see Karatzas & Shreve (1998). Their asymptotic properties have been analyzed by Björk & Näslund (1998), Hofmann & Platen (2000), Platen (2004a) and Guan, Liu & Chong (2004). Additionally, a notion of diversification in a particular modern portfolio sense can be found in Fernholz (2002).

We consider DPs under the *benchmark approach* described in Platen (2002) and (2004b). This concept is related to the notion of a *growth optimal portfolio* (GOP). The GOP is defined as the portfolio that maximizes expected logarithmic utility from terminal wealth, see Kelly (1956). The GOP is the best performing portfolio in the long run and can be used in derivative pricing, risk management and portfolio optimization. It appears in a wide range of literature including, for instance, Long (1990), Artzner (1997), Bajeux-Besnainou & Portait (1997), Karatzas & Shreve (1998), Kramkov & Schachermayer (1999), Becherer (2001), Platen (2002) and Goll & Kallsen (2003).

In practice, it is difficult to construct proxies of the GOP based on estimates of risk premia. It is, in principle, not possible to estimate any drift parameter with sufficient significance to be useful in sample based portfolio optimization, see Fama & French (2003) and DeMiguel, Garlappi & Uppal (2009). However, the Diversification Theorem proved in Platen (2005), shows that for a sequence of regular *jump diffusion financial markets*, any sequence of DPs is a sequence of approximate GOPs. This allows one in practice to approximate the GOP by any well diversified global market index.

This paper aims to demonstrate the robustness of the Diversification Theorem by simulating the GOP and DPs under various continuous financial market models. We emphasize that these simulations are exact or almost exact. The only approximation we allow is the approximation of integrals with respect to functions of finite variation. This avoids typical problems of stochastic numerical simulation as questions related to the non-Lipschitzness of coefficients, numerical stability and potential negative values for positive processes, propagation of errors, etc.. By focusing on almost exact simulations we make our results much more reliable than is typically achieved when using discrete time approximations of SDEs based on various schemes. The simulation results presented here give an impression about the closeness of DPs to the GOP when these are constructed from real market data, see, for instance, Platen & Rendek (2008).

We will simulate asset prices with dynamics modeled by the multi-asset Black-Scholes model, see Black & Scholes (1973); the multi-asset Heston model, see

Heston (1993); the multi-asset ARCH-diffusion model, see Nelson (1990) and Frey (1997); the multi-asset geometric Ornstein-Uhlenbeck volatility model, see Wiggins (1987) or Föllmer & Schweizer (1993); and the multi-currency minimal market model, see Platen (2001). These examples will illustrate the robustness of the diversification effect. The simulation studies will confirm that the convergence behavior of DPs towards the GOP appears to be largely model independent. This provides an important robustness property for applications of the benchmark approach. Finally, the paper makes the observation that for models, where the primary security accounts when expressed in units of the GOP are strict supermartingales, a well diversified portfolio, like the equal value weighted portfolio, significantly outperforms the typical market portfolio in the long run.

This paper is structured as follows. Section 2 defines DPs in a continuous financial market. Sections 3-8 describe exact or almost exact simulation of continuous financial market models. These sections also include simulation study of DPs under various model dynamics. In Section 3 we consider the multi-asset Black-Scholes model dynamics; in Section 4 the multi-asset Heston model dynamics; in Section 5 the multi-asset ARCH diffusion model dynamics; in Section 6 the multi-asset geometric Ornstein-Uhlenbek volatility model dynamics; in Section 7 the multi-currency minimal market model; and, finally, in Section 8 the multi-currency generalized minimal market model dynamics. Section 9 concludes.

# 2 Diversified Portfolios

Given a filtered probability space $(\Omega, \mathcal{A}, \underline{\mathcal{A}}, P)$, where $\underline{\mathcal{A}} = (\mathcal{A}_t)_{t\in[0,\infty)}$ is the filtration which satisfies the usual conditions, we consider markets with continuous security prices. *Trading uncertainty* is modeled by independent standard $(\underline{\mathcal{A}}, P)$-Wiener processes $W^k = \{W_t^k, t \in [0,\infty)\}$, for $k \in \{1, 2, \dots, d\}$ and $d \in \{1, 2, \dots\}$.

We consider a sequence of continuous financial market (CFM) models $\mathcal{S}_{(d)}^C$ indexed by a number $d \in \{1, 2, \dots\}$. For given $d$ the corresponding CFM comprises $d+1$ *primary security accounts*, denoted by $S_{(d)}^0, S_{(d)}^1, \dots, S_{(d)}^d$. These include a *savings account* $S_{(d)}^0 = \{S_{(d)}^0(t), t \in [0,\infty)\}$, which is the *locally riskless* primary security account expressed by

$$S_{(d)}^0(t) = \exp\left\{\int_0^t r_s ds\right\} < \infty \tag{2.1}$$

for $t \in [0,\infty)$, where $r = \{r_t, t \in [0,\infty)\}$ denotes the adapted *short rate.*

As shown in Platen & Heath (2006), in the $d$th CFM $\mathcal{S}_{(d)}^C$ there exists a unique GOP $S_{(d)}^{\delta_*} = \{S_{(d)}^{\delta_*}(t), t \in [0,\infty)\}$. The $d$th GOP is a strictly positive portfolio that maximizes the expected log-utility from terminal wealth, that is $E\left(\ln\left(S_{(d)}^{\delta}(T)\right)\right)$ for any $T \in [0,\infty)$, over all strictly positive portfolios $S_{(d)}^{\delta}$ for $d \in \{1, 2, \dots\}$, see Kelly (1956). It is a central object in the $d$th financial market $\mathcal{S}_{(d)}^{C}$ with outstanding mathematical properties.

In particular, one can use the GOP as *benchmark*. Let us, therefore, define the $j$th sequence of *benchmarked primary security account* processes $\hat{S}_{(d)}^{j} = \{\hat{S}_{(d)}^{j}(t), t \in [0,\infty)\}$ by the ratio

$$\hat{S}_{(d)}^{j}(t) = \frac{S_{(d)}^{j}(t)}{S_{(d)}^{\delta_*}(t)} \tag{2.2}$$

for $t \in [0,\infty)$ and $j \in \{0,1,\dots,d\}$, $d \in \{1,2,\dots\}$.

We also define a benchmarked portfolio process $\hat{S}_{(d)}^{\delta} = \{\hat{S}_{(d)}^{\delta}(t), t \in [0,\infty)\}$ in $\mathcal{S}_{(d)}^{C}$, where its value at time $t$ is given by

$$\hat{S}_{(d)}^{\delta}(t) = \sum_{j=0}^{d} \delta_t^j \hat{S}_{(d)}^{j}(t). \tag{2.3}$$

The *self-financing* property of this portfolio is visible in the form of the following stochastic differential equation (SDE)

$$d\hat{S}_{(d)}^{\delta}(t) = \sum_{j=0}^{d} \delta_t^j d\hat{S}_{(d)}^{j}(t) \tag{2.4}$$

for $t \in [0,\infty)$. Here, the vector of process of the predictable number of units invested $\boldsymbol{\delta} = \{\boldsymbol{\delta}_t = (\delta_t^0, \delta_t^1, \dots, \delta_t^d)^\top, t \in \Re^+\}$ represents the corresponding *strategy*, if the Itô integral

$$\int_0^t \delta_s^j d\hat{S}_{(d)}^{j}(s) \tag{2.5}$$

exists for all $j \in \{0,1,\dots,d\}$, $d \in \{1,2,\dots\}$ and $t \in [0,\infty)$.

All strategies and portfolios we will consider are self-financing. Moreover, since self-financing portfolios can, in general, become zero or negative in value, we consider in the following portfolios which are strictly positive.

Furthermore, we define for $\mathcal{S}_{(d)}^{C}$ the *fraction* $\pi_{\delta,t}^{j}$ of $\hat{S}_{(d)}^{\delta}(t)$ that is invested in the $j$th benchmarked primary security account $\hat{S}_{(d)}^{j}(t)$, $j \in \{1,2,\dots,d\}$, at time $t$, which is given by the formula

$$\pi_{\delta,t}^{j} = \delta_t^j \frac{\hat{S}_{(d)}^{j}(t)}{\hat{S}_{(d)}^{\delta}(t)} \tag{2.6}$$

for $j \in \{1,2,\dots,d\}$. Note that fractions can be negative but always sum to one, that is

$$\sum_{j=0}^{d} \pi_{\delta,t}^{j} = 1 \tag{2.7}$$

for $t \in [0, \infty)$.

Let us now describe potential proxies for the GOP. For a sequence of CFMs $\left(\mathcal{S}^C_{(d)}\right)_{d\in\{1,2,\dots\}}$ we call a corresponding sequence $\left(S^\delta_{(d)}\right)_{d\in\{1,2,\dots\}}$ of strictly positive portfolio processes $S^\delta_{(d)}$ a sequence of diversified portfolios (DPs) if some constants $K_1, K_2 \in (0,\infty)$ and $K_3 \in \{1,2,\dots\}$ exist, independently of $d$, such that for $d \in \{K_3, K_3+1, \dots\}$ the inequality

$$|\pi^j_{\delta,t}| \leq \frac{K_2}{d^{\frac{1}{2}+K_1}} \tag{2.8}$$

holds almost surely for all $j \in \{0,1,\dots,d\}$ and $t \in [0,\infty)$. This means that for a DP the fractions decline sufficiently fast for increasing $d$ but need not to be equal.

We need to assume that in a given sequence of CFMs the primary security accounts are sufficiently different. Otherwise, one cannot expect that any diversification is possible in the market under consideration. To achieve a sufficiently regular market let us ensure that each of the independent sources of trading uncertainty influences only a restricted range of benchmarked primary security accounts. More precisely, we assume the following regularity condition:

$$E\left((\hat{\sigma}^k_{(d)}(t))^2\right) \leq K_5 \tag{2.9}$$

for all $t \in [0,\infty)$, $d \in \{1,2,\dots\}$, $k \in \{1,2,\dots,d\}$ and a constant $K_5 \in (0,\infty)$. Here $\hat{\sigma}^k_{(d)}(t)$ is referred to as the $k$-th *total specific volatility* for $\mathcal{S}^C_{(d)}$ and is defined by the sum

$$\hat{\sigma}^k_{(d)}(t) = \sum_{j=0}^{d} |\sigma^{j,k}_{(d)}(t)| \tag{2.10}$$

for $k \in \{1,2,\dots\}$. The $(j,k)$th *specific volatility* $\sigma^{j,k}_{(d)}$, is the volatility of the $j$th benchmarked primary security account with respect to the $k$th source of trading uncertainty, see Platen & Heath (2006).

Furthermore, to measure the distance between an approximating portfolio $S^\delta_{(d)}$ and the GOP $S^{\delta_*}_{(d)}$ we define the *tracking rate* $R^\delta_{(d)}(t)$ at time $t$ by

$$R^\delta_{(d)}(t) = \sum_{k=1}^{d} \left( \sum_{j=0}^{d} \pi^j_{\delta,t} \sigma^{j,k}_{(d)}(t) \right)^2 \tag{2.11}$$

for $t \in [0,\infty)$. Note that one can show that the tracking rate vanishes when $S^\delta_{(d)}$ equals $S^{\delta_*}_{(d)}$. This is simply the consequence of the fact that the benchmarked GOP is a constant and, thus, has zero returns.

For a sequence $\left(\mathcal{S}^C_{(d)}\right)_{d\in\{1,2,\dots\}}$ of CFMs a sequence of strictly positive portfolios $\left(S^\delta_{(d)}\right)_{d\in\{1,2,\dots\}}$ is called a *sequence of approximate* GOPs when the corresponding sequence of tracking rates vanishes in probability, that is

$$\lim_{d\to\infty} R^{\delta}_{(d)}(t) = 0 \tag{2.12}$$

for all $t \in [0, \infty)$.

In reality one observes that well diversified, global stock portfolios behave very similar. This can be mathematically verified without imposing any major modeling assumptions. The *Diversification Theorem* proved in Platen (2005), shows that for a regular sequence of CFMs, see (2.9), any sequence of DPs is a sequence of approximate GOPs. Moreover, for any $d \in \{K_3, K_3 + 1, \dots\}$ and $t \in [0, \infty)$, the expected tracking rate of a given DP can be shown to satisfy the estimate

$$E\left(R^{\delta}_{(d)}(t)\right) \le \frac{(K_2)^2 K_5}{d^{2K_1}}. \tag{2.13}$$

Here, $K_1, K_2, K_5 \in (0, \infty)$ and $K_3 \in \{1, 2, \dots\}$.

This theorem is similar to the Law of Large Numbers and of practical significance. It allows us to approximate the GOP by any diversified global market index. It is very important to note that this result is model independent. It states that approximation of the GOP can be achieved by avoiding any calculation of the exact theoretical GOP fractions. This allows to overcome in practice the problem of risk premia which is, in principle, not possible with sufficient significance to be useful in portfolio optimization, see Fama & French (2003) and DeMiguel, Garlappi & Uppal (2009). By the Diversification Theorem one obtains proxies for the GOP in a robust manner as will be discussed in Sections 3-8.

In the following sections we illustrate the robustness of the diversification effect by simulation of diversified portfolios for various market models. By exploiting the nature of the market dynamics considered the simulation will be performed exactly or almost exactly. This is highly important since we want to study the diversification phenomenon over long periods of time.

To keep the presentation simple and transparent we consider in this paper only two types of indices, *market capitalization weighted indices* (MCIs) and *equally weighted indices* (EWIs). The indices constructed in this study are all self-financing portfolios. We characterize the indices in terms of fractions as in (2.6). For an MCI we define the fraction of wealth held in the $j$th constituent at time $t_n$ by the ratio

$$\pi^j_{\delta_{MCI},t_n} = \frac{\delta^j_{MCI,t_n}\, S^j_{t_n}}{\sum_{i=1}^d \delta^i_{MCI,t_n}\, S^i_{t_n}}, \tag{2.14}$$

for $j \in \{1, 2, \dots, d\}$, where $\delta^j_{MCI,t_n}$ denotes the number of units of the $j$th constituent available in the market at time $t_n$. An equally weighted index EWI is obtained by setting all fractions equal at the beginning of each trading period. The $j$th fraction of an EWI is then simply given by the constant ratio

$$\pi^j_{\delta_{EWI},t_n} = \frac{1}{d} \tag{2.15}$$

for $j = \{1, 2, \ldots, d\}$. Given the respective fractions, the value of a portfolio at time $t_n$ is recursively obtained according to the relation

$$S^{\delta}_{t_n} = S^{\delta}_{t_{n-1}} \left( 1 + \sum_{j=1}^{d} \pi^{j}_{\delta, t_{n-1}} \frac{S^{j}_{t_n} - S^{j}_{t_{n-1}}}{S^{j}_{t_{n-1}}} \right) \tag{2.16}$$

or equivalently

$$S^{\delta}_{t_n} = S^{\delta}_{t_{n-1}} + \sum_{j=1}^{d} \delta^{j}_{t_{n-1}} \left( S^{j}_{t_n} - S^{j}_{t_{n-1}} \right). \tag{2.17}$$

According to a given marked dynamics we simulate for the long period of $T = 150$ years the benchmarked trajectories of $d + 1 = 1001$ primary security accounts, sampling twice a week. For simplicity we set the interest rate to zero. Thus, the inverse of the benchmarked savings account provides the GOP when denominated in domestic currency, that is

$$S^{\delta_*}_{t} = (\hat{S}^{0}_{t})^{-1}. \tag{2.18}$$

The product of the GOP with the $j$th benchmarked primary security account yields the value of the $j$th primary security account denominated in domestic currency, that is,

$$S^{j}_{t} = \hat{S}^{j}_{t} S^{\delta_*}_{t}, \tag{2.19}$$

for $j \in \{0, 1, \ldots, d\}$. The initial values $S^{j}_{0}$, $j \in \{0, 1, \ldots, d\}$, are generated according to a Pareto distribution with parameters $\lambda = 1.1$ and $x_0 = \frac{\lambda - 1}{\lambda}$, see Simon (1958). For each model we plot the first 20 benchmarked primary security account processes in the respective figures in Sections 3-8. We also give an impression about the typical squared volatility process in these sections. Moreover, we plot for each market dynamics the simulated GOP as well as the EWI and the MCI, constructed from the simulated primary security accounts as described in (2.19). Additionally, we display in a separate figure for each market dynamics the benchmarked EWI and the benchmarked MCI. The benchmarked GOP is simply the constant one.

# 3 Multi-asset Black-Scholes Model

In this paper we use exact or almost exact simulation techniques for solutions of SDEs. When using discrete time numerical schemes for simulation there may be issues when dealing with non-Lipschitz continuous drift or diffusion coefficients. Also problems concerning numerical stability may arise or negative values could be obtained for strictly positive processes. Therefore, we describe in the following sections methods of exact and almost exact simulation of various market models, which avoid in principle, most of these problems. For simplicity, this presentation describes simulation methods for independent benchmarked primary security accounts. However, the case of dependent benchmarked primary security accounts

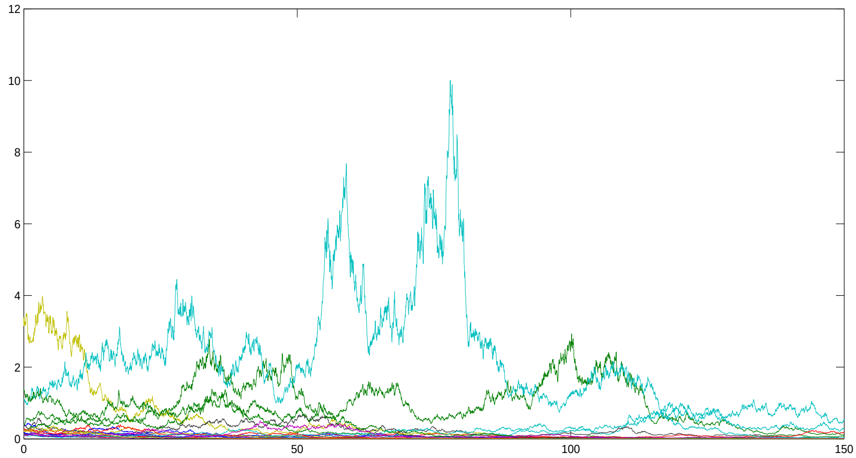


Figure 3.1: Simulated benchmarked primary security accounts under the Black-Scholes model

can be handled analogously. For details on simulation of correlated assets we refer to Platen & Rendek (2009).

Let us first describe the standard market model, which is the multi-asset Black-Scholes model, see Black & Scholes (1973). Under this model the benchmarked primary security accounts can be represented by the following matrix SDE

$$d\hat{\boldsymbol{S}}_t = \sum_{k=1}^{d} \boldsymbol{B}^k \hat{\boldsymbol{S}}_t dW_t^k, \tag{3.1}$$

for $t \in [0,\infty)$. Here $\hat{\boldsymbol{S}} = \{\hat{\boldsymbol{S}}_t = (\hat{S}_t^0, \hat{S}_t^1, \ldots, \hat{S}_t^d)^\top, t \in [0,\infty)\}$ is a vector of benchmarked primary security accounts, and $\boldsymbol{B}^k = [B^{k,i,j}]_{i,j=1}^d$ is a $d \times d$ diagonal parameter matrix, with elements

$$B^{k,i,j} = \begin{cases} b^{j,k} & \text{for} \quad i = j \\ 0 & \text{otherwise} \end{cases} \tag{3.2}$$

for $k, i, j \in \{1, 2, \ldots, d\}$. Note that $\hat{S}^j$, $j \in \{1, 2, \ldots, d\}$ forms here a martingale.

The multi-asset Black-Scholes model can be simulated exactly. The matrix SDE (3.1) has an exact solution, see Platen & Heath (2006). The $j$th benchmarked primary security accounts can be represented by

$$\hat{S}_t^j = \hat{S}_0^j \exp\left\{ -\frac{1}{2} \sum_{k=1}^{d} \left(b^{j,k}\right)^2 t + \sum_{k=1}^{d} b^{j,k} W_t^k \right\}. \tag{3.3}$$

Therefore, for the time discretization $0 < t_0 < t_1 < \cdots < \infty$, where $t_i = \Delta i$,

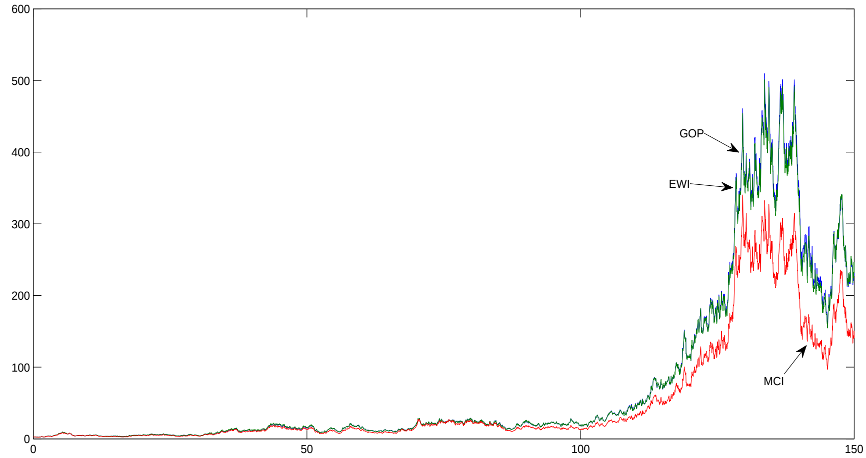


Figure 3.2: Simulated GOP, EWI and MCI under the Black-Scholes model

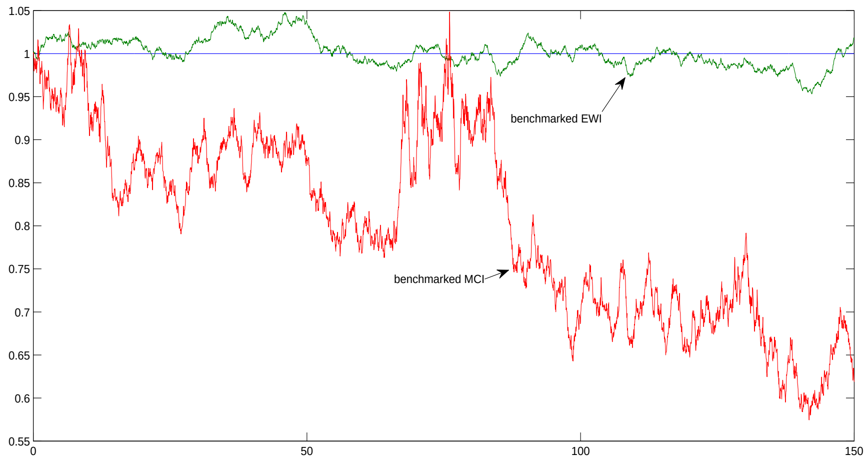


Figure 3.3: Simulated benchmarked GOP, EWI and MCI under the Black-Scholes model

$i \in \{0, 1, \dots\}$, we obtain the exponential

$$\hat{S}^j_{t_{i+1}} = \hat{S}^j_0 \exp\left\{ -\frac{1}{2}\left(b^{j,j}\right)^2 t_{i+1} + b^{j,j} W^j_{t_{i+1}} \right\} \tag{3.4}$$

for the $j$th independent benchmarked primary security account under the Black-Scholes model.

Let us now illustrate the fundamental phenomenon of diversification by simulating in a Black-Scholes market diversified portfolios. This can be exactly performed without any error as described above. We simulate 1001 independent benchmarked primary security accounts with $b^{j,j} = 0.2$ for $j \in \{0, 1, \ldots, 1000\}$ according to (3.4) end display the first 20 resulting trajectories in Fig. 3.1. We emphasize that these benchmarked primary security accounts are here martingales. Here, the independent initial value $\hat{S}_0^j$ is generated using the Pareto distribution with parameters $\lambda = 1.1$ and $x_0 = \frac{\lambda - 1}{\lambda}$, see Simon (1958). This models the fact that there is a great variety in the market capitalization of stocks.

In Fig 3.2 we show the simulated GOP, the EWI and the MCI. In this case the EWI approximates rather well the GOP. The MCI seems to be initially a good proxy of the GOP, however after this initial time period it diverges from the GOP. Most likely some large stock values emerge and the resulting large fractions of these stocks distort the performance of the market index. These fractions of the corresponding primary security accounts are simply to large to be acceptable as those of a DP and, thus violate the conditions of the Diversification Theorem. This phenomenon is also illustrated in Fig. 3.3 where we display the benchmarked GOP, $\hat{S}_t^{\delta_*} = 1$, as well as the benchmarked EWI simulated under the Black-Scholes model and the benchmarked MCI constructed from 1000 benchmarked primary security accounts. Note that initially in the first 10 years, sometimes the benchmarked EWI, sometimes the benchmarked MCI performed better. However, in the long term simulation we clearly see that the benchmarked EWI converges in the long run to the benchmarked GOP, while the benchmarked MCI tends downwards. In this figure we also note that the benchmarked MCI has much larger variance then the benchmarked EWI.

# 4 Multi-asset Heston Model

The Heston model, see Heston (1993), can be described by a set of two matrix SDEs in the form

$$d\hat{\boldsymbol{S}}_t = \mathrm{diag}\left(\sqrt{\boldsymbol{V}_t}\right) \mathrm{diag}\left(\hat{\boldsymbol{S}}_t\right) \left(\boldsymbol{A} d\tilde{\boldsymbol{W}}_t^1 + \boldsymbol{B} d\tilde{\boldsymbol{W}}_t^2\right), \tag{4.1}$$

$$d\boldsymbol{V}_t = (\boldsymbol{a} - \boldsymbol{E}\boldsymbol{V}_t)\, dt + \boldsymbol{F} \mathrm{diag}\left(\sqrt{\boldsymbol{V}_t}\right) d\tilde{\boldsymbol{W}}_t^1, \tag{4.2}$$

for $t \in [0, \infty)$. Here $\hat{\boldsymbol{S}} = \{\hat{\boldsymbol{S}}_t = (\hat{S}_t^0, \hat{S}_t^1, \ldots, \hat{S}_t^d)^\top, t \in [0, \infty)\}$ is a vector of benchmarked primary security accounts which are supermartingales, see Platen & Heath (2006). Moreover, $\tilde{\boldsymbol{W}}^1 = \{\tilde{\boldsymbol{W}}_t^1 = (\tilde{W}_t^{1,1}, \tilde{W}_t^{1,2}, \ldots, \tilde{W}_t^{1,d})^\top, t \in [0, \infty)\}$ and $\tilde{\boldsymbol{W}}^2 = \{\tilde{\boldsymbol{W}}_t^2 = (\tilde{W}_t^{2,1}, \tilde{W}_t^{2,2}, \ldots, \tilde{W}_t^{2,d})^\top, t \in [0, \infty)\}$ are independent vectors of correlated Wiener processes. That is

$$\tilde{\boldsymbol{W}}_t^k = \boldsymbol{C}^k \boldsymbol{W}_t^k, \tag{4.3}$$

where $\boldsymbol{C}^k = [C^{k,i,j}]_{i,j=1}^d$ and $\boldsymbol{W}^k = \{\boldsymbol{W}_t^k = (W_t^{k,1}, W_t^{k,2}, \ldots, W_t^{k,d})^\top, t \in [0, \infty)\}$, $k \in \{1, 2\}$ is again a vector of independent Wiener processes.

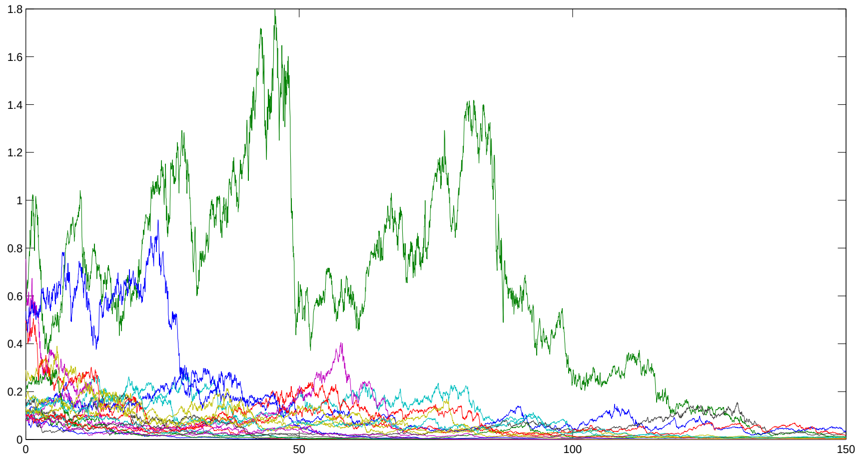

Figure 4.1: Simulated benchmarked primary security accounts under the Heston model

Additionally, $\boldsymbol{A} = [A^{i,j}]_{i,j=1}^{d}$ is a diagonal matrix with elements

$$A^{i,j} = \begin{cases} \varrho_i & \text{for} \quad i = j \\ 0 & \text{otherwise} \end{cases} \tag{4.4}$$

and $\boldsymbol{B} = [B^{i,j}]_{i,j=1}^{d}$ is a diagonal matrix with elements

$$B^{i,j} = \begin{cases} \sqrt{1-\varrho_i^2} & \text{for} \quad i = j \\ 0 & \text{otherwise.} \end{cases} \tag{4.5}$$

Moreover, $\boldsymbol{V} = \{\boldsymbol{V}_t = (V_t^1, V_t^2, \ldots, V_t^d)^\top, t \in [0,\infty)\}$ is a vector of squared volatilities, $\boldsymbol{a} = (a_1, a_2, \ldots, a_d)^\top$; and $\boldsymbol{E} = [E^{i,j}]_{i,j=1}^{d}$ is a diagonal matrix with elements

$$E^{i,j} = \begin{cases} \kappa_i & \text{for} \quad i = j \\ 0 & \text{otherwise,} \end{cases} \tag{4.6}$$

and $\boldsymbol{F} = [F^{i,j}]_{i,j=1}^{d}$ is a diagonal matrix with elements

$$F^{i,j} = \begin{cases} \gamma_i & \text{for} \quad i = j \\ 0 & \text{otherwise.} \end{cases} \tag{4.7}$$

One method for the exact simulation of the Heston model has been discussed in Broadie & Kaya (2006). We use here a simplified almost exact simulation of the benchmarked primary security accounts under the Heston model. This method involves exact simulation of the squared volatility processes and almost exact simulation of the independent benchmarked primary security accounts, given the trajectories of the squared volatilities as explained in Platen & Rendek (2009).

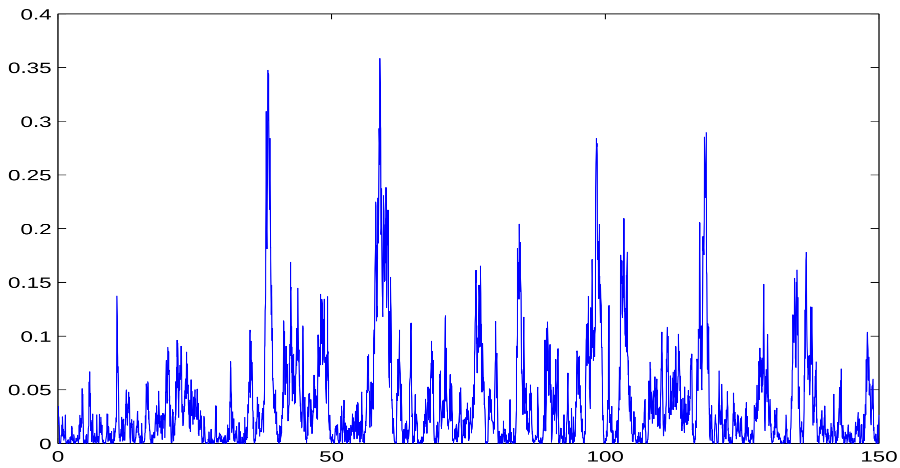


Figure 4.2: Simulated squared volatility under the Heston model

We obtain the value of the $j$th squared volatility $V^j_{t_{i+1}}$ at time $t_{i+1}$, $i \in \{0, 1, \dots\}$, by sampling directly from the noncentral chi-square distribution $\chi'^2_{\nu_j}(\lambda_j)$ with $\nu_j$ degrees of freedom and noncentrality parameter $\lambda_j$. That is

$$V^j_{t_{i+1}} = \frac{\gamma_j^2 \left(1 - \exp\{-\kappa_j \Delta\}\right)}{4\kappa_j} \chi'^2_{\nu_j} \left( \frac{4\kappa_j e^{-\kappa_j \Delta}}{\gamma_j^2 \left(1 - e^{-\kappa_j \Delta}\right)} V^j_{t_i} \right), \tag{4.8}$$

where $\nu_j = \frac{4a_j}{\gamma_j^2}$. Sampling from the noncentral chi-square distribution is discussed, for instance, in Glasserman (2004). The resulting simulation method for $V^j$ is exact.

Let us now describe the almost exact simulation of the vector of logarithms of the benchmarked assets $\boldsymbol{X}_t = \ln(\hat{\boldsymbol{S}}_t)$. Following Broadie & Kaya (2006) we may represent the $j$th value of $X^j_{t_{i+1}}$ at time $t_{i+1}$ in the form

$$\begin{aligned} X^j_{t_{i+1}} &= X^j_{t_i} + \frac{\varrho_j}{\gamma_j}\left(V^j_{t_{i+1}} - V^j_{t_i} - a_j \Delta\right) + \left(\frac{\varrho_j \kappa_j}{\gamma_j} - \frac{1}{2}\right) \int_{t_i}^{t_{i+1}} V^j_u du \\ &\quad + \sqrt{1 - \varrho_j^2} \int_{t_i}^{t_{i+1}} \sqrt{V^j_u} dW^{2,j}_u. \end{aligned} \tag{4.9}$$

Furthermore, the distribution of

$$\int_{t_i}^{t_{i+1}} \sqrt{V^j_u} dW^{2,j}_u, \tag{4.10}$$

given the path of $V^j$, is Gaussian with mean zero and variance $\int_{t_i}^{t_{i+1}} V^j_u du$, since $V^j$ is independent of the Brownian motion $W^{2,j}$ for all $j \in \{1, 2, \dots, d\}$. Moreover,

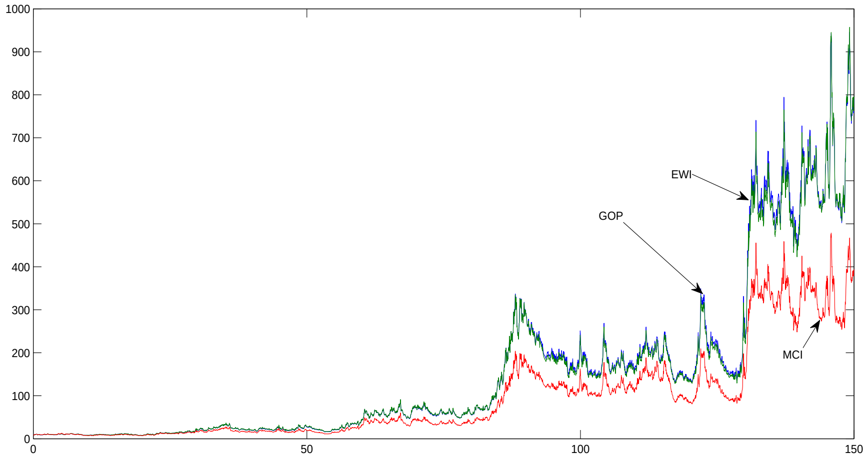


Figure 4.3: Simulated GOP, EWI and MCI under the Heston model

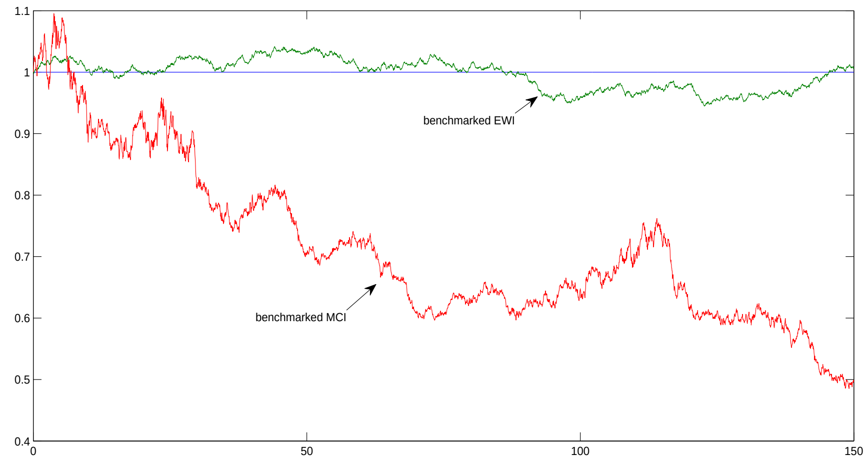


Figure 4.4: Simulated benchmarked GOP, EWI and MCI under the Heston model

it is possible to approximate $\int_{t_i}^{t_{i+1}} V_u^j du$ given the path of the process $V^j$. We use here the well known trapezoidal rule

$$\int_{t_i}^{t_{i+1}} V_u^j du \approx \frac{\Delta}{2}\left(V_{t_i}^j + V_{t_{i+1}}^j\right). \tag{4.11}$$

Consequently,

$$\int_{t_i}^{t_{i+1}} \sqrt{V_u^j} dW_u^{2,j} \approx \mathcal{N}\left(0, \frac{\Delta}{2}\left(V_{t_i}^j + V_{t_{i+1}}^j\right)\right). \tag{4.12}$$

This approximation can be achieved with high accuracy, by the above quadrature formula. For the multi-asset Heston model this results in an efficient almost exact simulation technique by conditioning.

We now use for the benchmarked primary security accounts the multi-asset Heston model with independent prices. We display the first 20 simulated independent benchmarked primary security accounts under the multi-asset Hestion model in Fig. 4.1. These benchmarked primary security accounts are supermartingales. The parameters in (4.8) are estimated by a Heston fit to the SPX surface as of the close on Sep 15, 2005, see Gatheral (2006). The $j$th squared volatility process is simulated according to (4.8) for initial value $V_0^j = 0.0174$, $a_j = 0.0469$, $\kappa_j = 1.3253$, $\gamma_j = 0.3877$, $j \in \{0, 1, \ldots, 1000\}$. The correlation parameter is here set to $\varrho_j = -0.7165$ in order to reflect the leverage effect, see Black (1976). The initial values $\hat{S}_0^j$ are again generated from the Pareto distribution. Additionally, we display in Fig. 4.2 a typical trajectory of the squared volatility process $V^j$ under the Heston model simulated exactly with the formula (4.8).

In Fig 4.3 we display the simulated GOP, EWI and MCI under the Heston model. Also here the EWI provides a good proxy for the GOP. The MCI however, does not perform as good as the GOP and the EWI. Additionally, in Fig. 4.4 we illustrate the benchmarked GOP, $\hat{S}_t^{\delta_*} = 1$, the benchmarked EWI and the benchmarked MCI obtained from 1000 benchmarked primary security accounts. This plot clearly shows the convergence of the benchmarked EWI to the benchmarked GOP. The benchmarked MCI, similar to the simulation under the Black-Scholes model, has downward trend.

# 5 Multi-asset ARCH-diffusion Model

The continuous time limits of some popular time series models in finance can be described by a multi-dimensional ARCH-diffusion model. The class of ARCH and GARCH time series models was originally proposed in Engle (1982). The ARCH diffusion model is obtained as a continuous time limit of the innovation process of the GARCH(1, 1) and NGARCH(1, 1) models, see Nelson (1990) and Frey (1997). The ARCH-diffusion model can be described by the following set of two matrix SDEs in the form

$$d\hat{\boldsymbol{S}}_t = \operatorname{diag}\left(\sqrt{\boldsymbol{V}_t}\right) \operatorname{diag}\left(\hat{\boldsymbol{S}}_t\right) \left(\boldsymbol{A} d\tilde{\boldsymbol{W}}_t^1 + \boldsymbol{B} d\tilde{\boldsymbol{W}}_t^2\right), \tag{5.1}$$

$$d\boldsymbol{V}_t = (\boldsymbol{a} - \boldsymbol{E}\boldsymbol{V}_t)\, dt + \boldsymbol{F} \operatorname{diag}(\boldsymbol{V}_t)\, d\tilde{\boldsymbol{W}}_t^1, \tag{5.2}$$

for $t \in [0, \infty)$. Here $\hat{\boldsymbol{S}} = \{\hat{\boldsymbol{S}}_t = (\hat{S}_t^0, \hat{S}_t^1, \ldots, \hat{S}_t^d)^\top, t \in [0, \infty)\}$ denotes again a vector of benchmarked primary security accounts which are supermartingales. Furthermore, $\tilde{\boldsymbol{W}}^1 = \{\tilde{\boldsymbol{W}}_t^1 = (\tilde{W}_t^{1,1}, \tilde{W}_t^{1,2}, \ldots, \tilde{W}_t^{1,d})^\top, t \in [0, \infty)\}$ and $\tilde{\boldsymbol{W}}^2 = \{\tilde{\boldsymbol{W}}_t^2 = (\tilde{W}_t^{2,1}, \tilde{W}_t^{2,2}, \ldots, \tilde{W}_t^{2,d})^\top, t \in [0, \infty)\}$ are independent vectors of correlated Wiener processes. Additionally, $\boldsymbol{A} = [A^{i,j}]_{i,j=1}^d$ is a diagonal matrix with elements

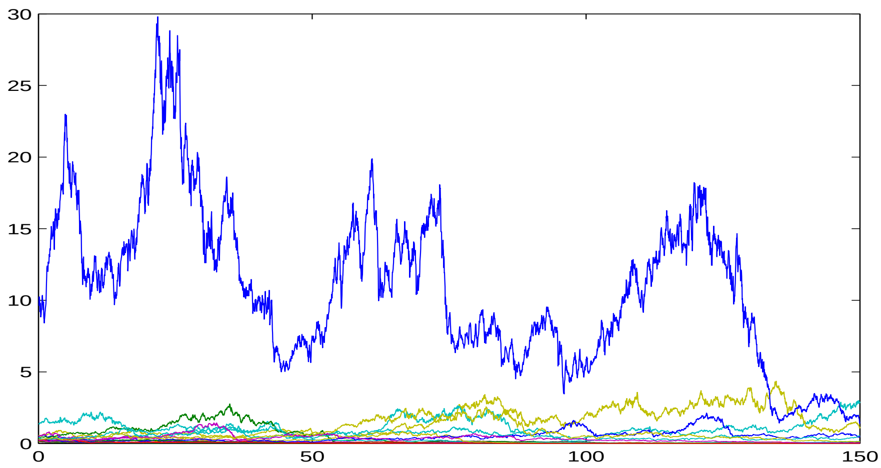


Figure 5.1: Simulated benchmarked primary security accounts under the ARCH-diffusion model

as in (4.4), and $\boldsymbol{B} = [B^{i,j}]_{i,j=1}^{d}$ is a diagonal matrix with elements (4.5). Moreover, $\boldsymbol{V} = \{\boldsymbol{V}_t = (V_t^1, V_t^2, \dots, V_t^d)^\top, t \in [0,\infty)\}$ is a vector of squared volatilities, $\boldsymbol{a} = (a_1, a_2, \dots, a_d)^\top$; $\boldsymbol{E} = [E^{i,j}]_{i,j=1}^{d}$ is a diagonal matrix with elements as in (4.6); and $\boldsymbol{F} = [F^{i,j}]_{i,j=1}^{d}$ is a diagonal matrix with elements as in (4.7).

In the given case we can simulate the $j$th squared volatility process $V^j$, $j \in \{0, 1, \dots\}$ almost exactly by approximating the time integral via the trapezoidal rule in the following exact representation

$$\begin{aligned} V_{t_{i+1}}^j &= \exp\left\{\left(-\kappa_j - \frac{1}{2}\gamma_j^2\right) t_{i+1} + \gamma_j W_{t_{i+1}}^{1,j}\right\} \\ &\quad \times \left(V_{t_0}^j + a_j \sum_{k=0}^{i} \int_{t_k}^{t_{k+1}} \exp\left\{\left(\kappa_j + \frac{1}{2}\gamma_j^2\right) s - \gamma_j W_s^{1,j}\right\} ds\right). \end{aligned} \tag{5.3}$$

This yields the approximation

$$\begin{aligned} V_{t_{i+1}}^{j\Delta} &= \exp\left\{\left(-\kappa_j - \frac{1}{2}\gamma_j^2\right) t_{i+1} + \gamma_j W_{t_{i+1}}^{1,j}\right\} \\ &\quad \times \left(V_{t_0}^j + a_j \frac{\Delta}{2} \sum_{k=0}^{i} \left[\exp\left\{\left(\kappa_j + \frac{1}{2}\gamma_j^2\right) t_k - \gamma_j W_{t_k}^{1,j}\right\}\right.\right. \\ &\quad \left.\left. + \exp\left\{\left(\kappa_j + \frac{1}{2}\gamma_j^2\right) t_{k+1} - \gamma_j W_{t_{k+1}}^{1,j}\right\}\right]\right) \end{aligned} \tag{5.4}$$

for $t_i = \Delta i, i \in \{0, 1, \dots\}$.

Let us now describe the almost exact simulation of the vector $\boldsymbol{X}_t = \ln\left(\hat{\boldsymbol{S}}_t\right)$. Following Platen & Rendek (2009), we may represent the $j$th value of $X_{t_{i+1}}^j$ at

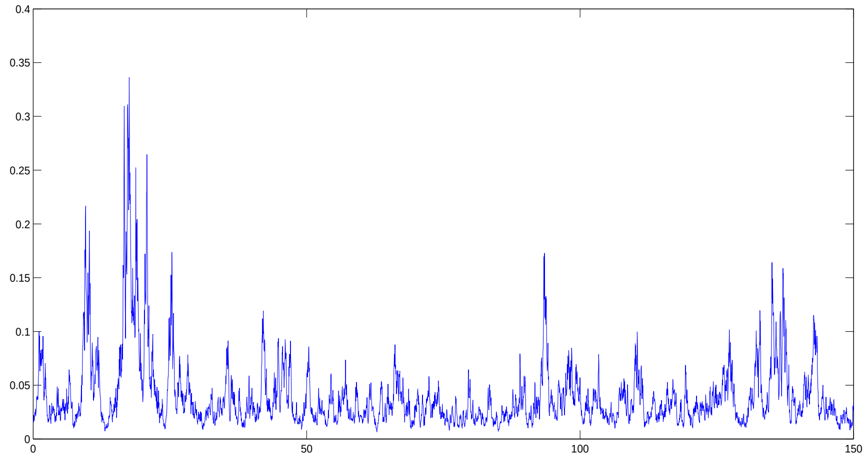


Figure 5.2: Simulated squared volatility under the ARCH-diffusion model

time $t_{i+1}$ in the following way:

$$\begin{aligned} X^j_{t_{i+1}} &= X^j_{t_i} - \frac{1}{2}\int_{t_i}^{t_{i+1}} V^j_u du + \frac{2\varrho_j}{\gamma_j}\left(\sqrt{V^j_{t_{i+1}}} - \sqrt{V^j_{t_i}}\right) \\ & \quad -\frac{2\varrho_j}{\gamma_j}\int_{t_i}^{t_{i+1}}\left(\frac{a_j}{2\sqrt{V^j_u}} - \left(\frac{\kappa_j}{2} + \frac{\gamma_j^2}{8}\right)\sqrt{V^j_u}\right) du \\ & \quad +\sqrt{1-\varrho_j^2}\int_{t_i}^{t_{i+1}}\sqrt{V^j_u}\, dW^{2,j}_u. \end{aligned} \tag{5.5}$$

Furthermore, the distribution of

$$\int_{t_i}^{t_{i+1}}\sqrt{V^j_u}\, dW^{2,j}_u, \tag{5.6}$$

conditioned on the path of $V^j$, is Gaussian with mean zero and variance $\int_{t_i}^{t_{i+1}} V^j_u du$, because $V^j$ is independent of the Brownian motion $W^{2,j}$ for all $j \in \{1, 2, \ldots, d\}$. Moreover, it is possible to approximate $\int_{t_i}^{t_{i+1}} V^j_u du$ given the path of the process $V^j$. We use here the following trapezoidal approximation

$$\int_{t_i}^{t_{i+1}} V^j_u du \approx \frac{\Delta}{2}\left(V^j_{t_i} + V^j_{t_{i+1}}\right) \tag{5.7}$$

to obtain

$$\int_{t_i}^{t_{i+1}}\sqrt{V^j_u}\, dW^{2,j}_u \approx \mathcal{N}\left(0, \frac{\Delta}{2}\left(V^j_{t_i} + V^j_{t_{i+1}}\right)\right). \tag{5.8}$$

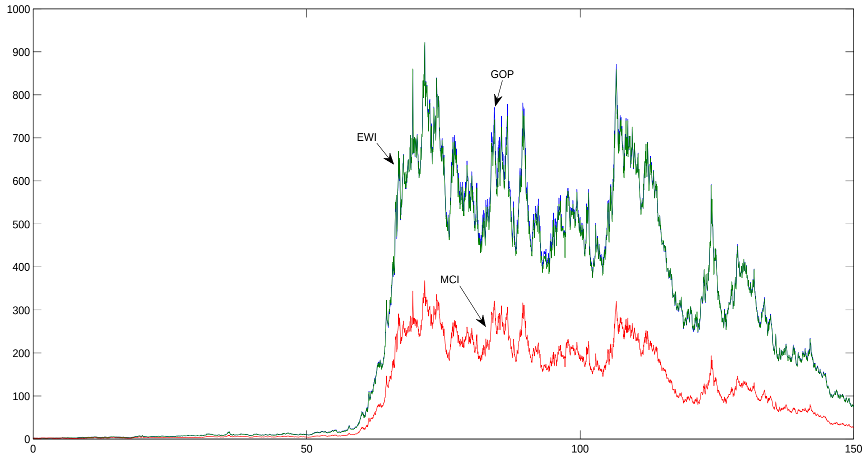


Figure 5.3: Simulated GOP, EWI and MCI under the ARCH-diffusion model

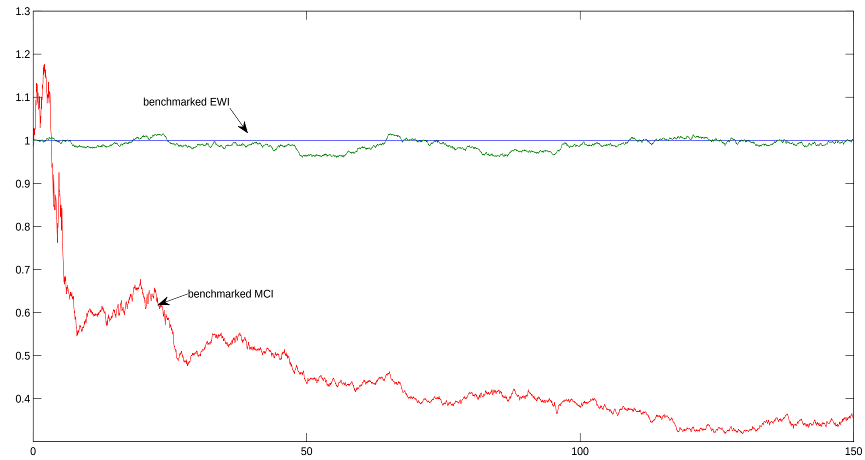


Figure 5.4: Simulated benchmarked GOP, EWI and MCI under the ARCH-diffusion model

Similarly, it is possible to approximate the integral in the form

$$\int_{t_i}^{t_{i+1}} \left( \frac{a_j}{2\sqrt{V_u^j}} - \left( \frac{\kappa_j}{2} + \frac{\gamma_j^2}{8} \right) \sqrt{V_u^j} \right) du \approx \tag{5.9}$$

$$\frac{\Delta}{2} \left( \frac{a_j}{2\sqrt{V_{t_i}^j}} - \left( \frac{\kappa_j}{2} + \frac{\gamma_j^2}{8} \right) \sqrt{V_{t_i}^j} + \frac{a_j}{2\sqrt{V_{t_{i+1}}^j}} - \left( \frac{\kappa_j}{2} + \frac{\gamma_j^2}{8} \right) \sqrt{V_{t_{i+1}}^j} \right).$$

This approximation can be achieved with high accuracy by using the simple

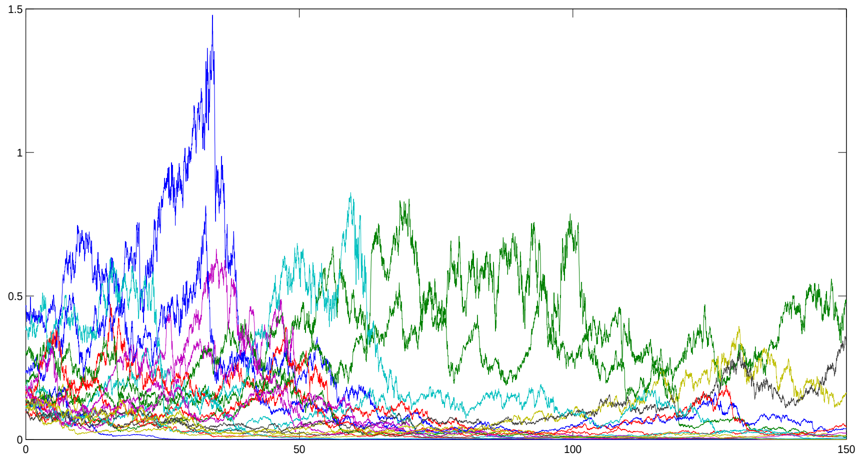


Figure 6.1: Simulated benchmarked primary security accounts under the geometric Ornstein-Uhlenbeck volatility model

quadrature formula. We obtain an efficient almost exact simulation technique by conditioning for the multi-asset ARCH-diffusion model.

Let us now simulate the benchmarked primary security accounts as a multi-dimensional ARCH diffusion, as described above. We make the squared volatility process the same for all benchmarked primary security accounts, where we set $a = 0.0469$, $\kappa = 1.3253$, $\gamma = 1$ and $V_0 = 0.0174$, as calibrated by comparison to the Heston squared volatility process. Furthermore, the driving noise of each of the benchmarked asset prices is independent from each other. It is, however, correlated with $\varrho = -0.7165$ to the corresponding squared volatility process. In Fig. 5.1 we show the first 20 resulting benchmarked risky primary security accounts. A typical trajectory of the squared volatility under the ARCH-diffusion model is displayed in Fig. 5.2.

The Fig. 5.3 display the corresponding GOP, EWI and MCI. Moreover, Fig. 5.4 exhibits the benchmarked GOP, $\hat{S}_t^{\delta_*} = 1$, the benchmarked EWI and the benchmarked MCI. Also here the EWI appears to be a very good proxy of the GOP, while the MCI does not come close enough to the GOP to be acceptable as a good proxy.

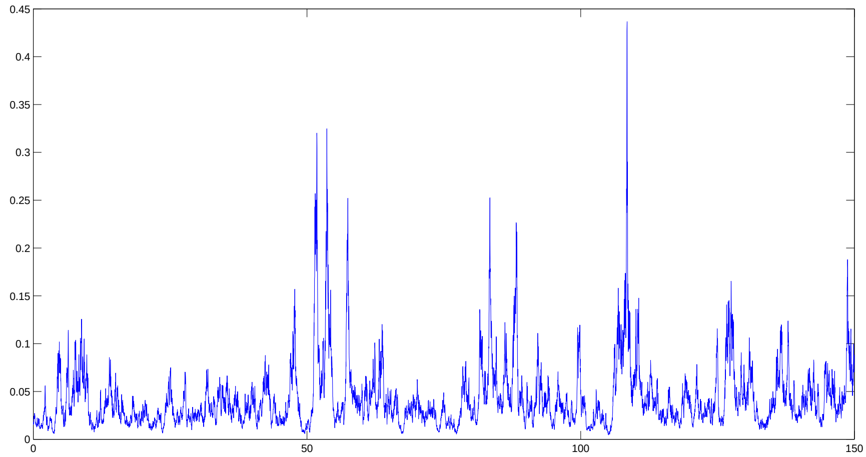


Figure 6.2: Simulated squared volatility under the geometric Ornstein-Uhlenbeck volatility model

# 6 Geometric Ornstein-Uhlenbeck Volatility Model

Similar as in the Heston and the ARCH-diffusion model we generate the benchmarked asset prices by using some stochastic volatility that is now a geometric Ornstein-Uhlenbeck process. The geometric Ornstein-Uhlenbeck volatility model can be described by the following set of two matrix SDEs in the form

$$d\hat{\boldsymbol{S}}_t = \mathrm{diag}\left(\exp\{\boldsymbol{V}_t\}\right)\mathrm{diag}\left(\hat{\boldsymbol{S}}_t\right)\left(\boldsymbol{A}d\tilde{\boldsymbol{W}}^1_t + \boldsymbol{B}d\tilde{\boldsymbol{W}}^2_t\right), \tag{6.1}$$

$$d\boldsymbol{V}_t = \left(\boldsymbol{a} - \boldsymbol{E}\boldsymbol{V}_t\right)dt + \boldsymbol{F}d\tilde{\boldsymbol{W}}^1_t, \tag{6.2}$$

for $t \in [0, \infty)$. Here $\hat{\boldsymbol{S}} = \{\hat{\boldsymbol{S}}_t = (\hat{S}^0_t, \hat{S}^1_t, \ldots, \hat{S}^d_t)^\top, t \in [0, \infty)\}$ denotes again a vector of benchmarked primary security accounts which are supermartingales. Furthermore, $\tilde{\boldsymbol{W}}^1 = \{\tilde{\boldsymbol{W}}^1_t = (\tilde{W}^{1,1}_t, \tilde{W}^{1,2}_t, \ldots, \tilde{W}^{1,d}_t)^\top, t \in [0, \infty)\}$ and $\tilde{\boldsymbol{W}}^2 = \{\tilde{\boldsymbol{W}}^2_t = (\tilde{W}^{2,1}_t, \tilde{W}^{2,2}_t, \ldots, \tilde{W}^{2,d}_t)^\top, t \in [0, \infty)\}$ are independent vectors of correlated Wiener processes. Additionally, $\boldsymbol{A} = [A^{i,j}]^d_{i,j=1}$ is a diagonal matrix with elements as in (4.4), and $\boldsymbol{B} = [B^{i,j}]^d_{i,j=1}$ is a diagonal matrix with elements (4.5). Moreover,

$$\exp\{\boldsymbol{V}\} = \left\{\exp\{\boldsymbol{V}_t\} = \left(\exp\{V^1_t\}, \exp\{V^2_t\}, \ldots, \exp\{V^d_t\}\right)^\top, t \in [0, \infty)\right\} \tag{6.3}$$

is a vector of volatilities, whose elements are correlated exponents of the Ornstein-Uhlenbeck processes. Additionally $\boldsymbol{a} = (a_1, a_2, \ldots, a_d)^\top$; $\boldsymbol{E} = [E^{i,j}]^d_{i,j=1}$ is a diagonal matrix with elements as in (4.6); and $\boldsymbol{F} = [F^{i,j}]^d_{i,j=1}$ is a diagonal matrix with elements as in (4.7).

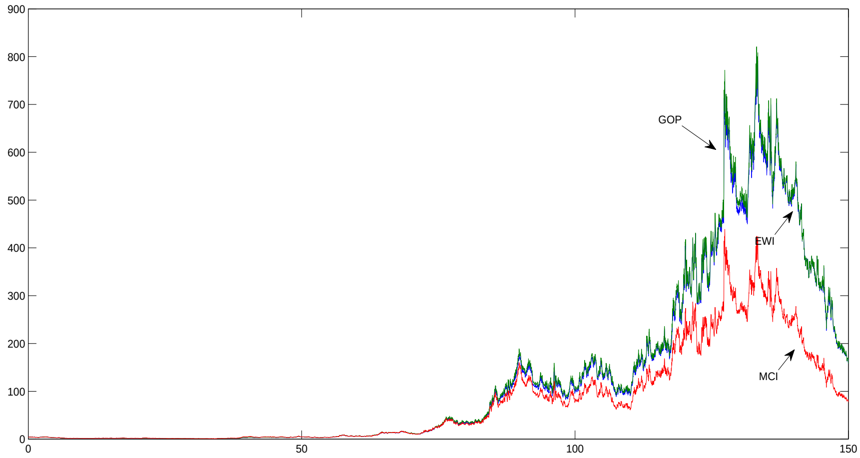


Figure 6.3: Simulated GOP, EWI and MCI under the geometric Ornstein-Uhlenbeck volatility model

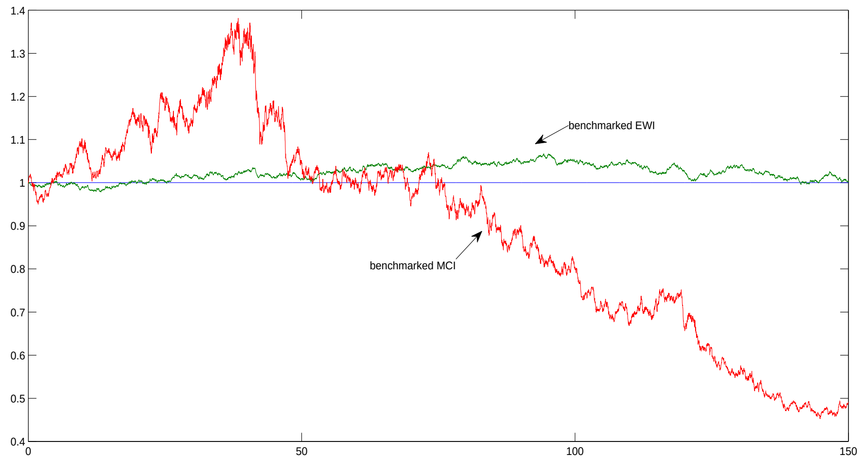


Figure 6.4: Simulated benchmarked GOP, EWI and MCI under the geometric Ornstein-Uhlenbeck volatility model

As before we consider simulation of independent benchmarked primary security accounts. We obtain the value of the $j$th volatility $\exp\left\{V_{t_i}^j\right\}$ at time $t_i$, $i \in \{0, 1, \dots\}$, by the following exact solution

$$\exp\{V_{t_i}^j\} = \exp\left\{V_0^j e^{-\kappa_j t_i} + \frac{a_j}{\kappa_j}\left(1 - e^{-\kappa_j t_i}\right) + \gamma_j e^{-\kappa_j t_i} \sum_{k=1}^{i} \int_{t_{k-1}}^{t_k} e^{\kappa_j s} dW_s^{1,j}\right\}. \tag{6.4}$$

Here

$$\int_{t_{k-1}}^{t_k} e^{\kappa_j s} dW_s^{1,j} \sim \mathcal{N}\left(0, \frac{1}{2\kappa}\left(e^{2\kappa_j t_k} - e^{2\kappa_j t_{k-1}}\right)\right). \tag{6.5}$$

The resulting simulation method for $\exp\{V^j\}$ is exact.

Let us now describe the almost exact simulation of the vector $\boldsymbol{X}_t = \ln\left(\hat{\boldsymbol{S}}_t\right)$. Again, following Platen & Rendek (2009), we may represent the $j$th value of $X_{t_{i+1}}^j$ at time $t_{i+1}$ in the following way:

$$\begin{aligned} X_{t_{i+1}}^j &= X_{t_i}^j - \frac{1}{2}\int_{t_i}^{t_{i+1}} e^{2V_u^j} du + \frac{\varrho_j}{\gamma_j}\left(e^{V_{t_{i+1}}^j} - e^{V_{t_i}^j}\right) \\ &\quad -\frac{\varrho_j}{\gamma_j}\int_{t_i}^{t_{i+1}}\left(\left(a_j + \frac{\gamma_j^2}{2}\right)e^{V_u^j} - \kappa_j V_u^j e^{V_u^j}\right) du \\ &\quad +\sqrt{1-\varrho_j^2}\int_{t_i}^{t_{i+1}} e^{V_u^j} dW_u^{2,j}. \end{aligned} \tag{6.6}$$

Furthermore, the distribution of

$$\int_{t_i}^{t_{i+1}} e^{V_u^j} dW_u^{2,j}, \tag{6.7}$$

conditioned on the path of $V^j$, is Gaussian with mean zero and variance $\int_{t_i}^{t_{i+1}} e^{2V_u^j} du$, because $V^j$ is independent of the Brownian motion $W^{2,j}$ for all $j \in \{1, 2, \ldots, d\}$. Moreover, it is possible to approximate $\int_{t_i}^{t_{i+1}} e^{2V_u^j} du$ given the path of the process $V^j$. We use here the following trapezoidal approximation

$$\int_{t_i}^{t_{i+1}} e^{2V_u^j} du \approx \frac{\Delta}{2}\left(e^{2V_{t_i}^j} + e^{2V_{t_{i+1}}^j}\right) \tag{6.8}$$

to obtain

$$\int_{t_i}^{t_{i+1}} e^{V_u^j} dW_u^{2,j} \approx \mathcal{N}\left(0, \frac{\Delta}{2}\left(e^{2V_{t_i}^j} + e^{2V_{t_{i+1}}^j}\right)\right). \tag{6.9}$$

Similarly, it is possible to approximate the integral in the form

$$\begin{aligned} &\int_{t_i}^{t_{i+1}}\left(\left(a_j + \frac{\gamma_j^2}{2}\right)e^{V_u^j} - \kappa_j V_u^j e^{V_u^j}\right) du \approx \\ &\frac{\Delta}{2}\left(\left(a_j + \frac{\gamma_j^2}{2}\right)e^{V_{t_i}^j} - \kappa_j V_{t_i}^j e^{V_{t_i}^j} + \left(a_j + \frac{\gamma_j^2}{2}\right)e^{V_{t_{i+1}}^j} - \kappa_j V_{t_{i+1}}^j e^{V_{t_{i+1}}^j}\right). \end{aligned} \tag{6.10}$$

This approximation can be achieved with high accuracy by using the simple quadrature formula. We obtain an efficient almost exact simulation technique by conditioning for the multi-asset geometric Ornstein-Uhlenbeck volatility model.

We now simulate the benchmarked primary security accounts from a multi-dimensional geometric Ornstein-Uhlenbeck volatility model, as described above.

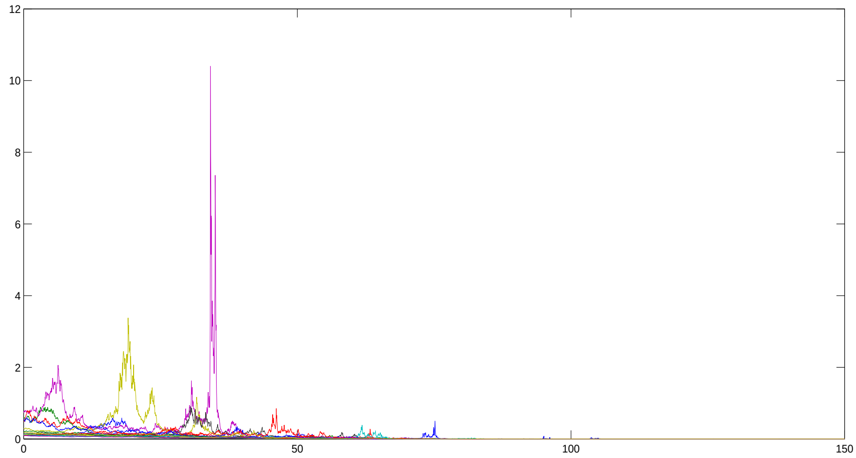


Figure 7.1: Simulated benchmarked primary security accounts under the MMM

We make the squared volatility process $e^{2V^j}$ calibrated by comparison to the Heston and the ARCH-diffusion squared volatility processes, where we set $a_j = -2.2143$, $\kappa_j = 1.3253$, $\gamma_j = 0.52$ and $V_0^j = -2.0257$, $j \in \{0, 1, \ldots, 1000\}$. Furthermore, the driving noise of each of the benchmarked asset prices is independent from each other. It is, however, correlated with $\varrho_j = -0.7165$ to the corresponding squared volatility process. In Fig. 6.1 we show the first 20 resulting benchmarked risky primary security accounts. A typical trajectory of the squared volatility under the geometric Ornstein-Uhlenbeck model is displayed in Fig. 6.2.

The Fig. 6.3 displays the corresponding GOP, EWI and MCI. Moreover, Fig. 6.4 exhibits the benchmarked GOP, $\hat{S}_t^{\delta_*} = 1$, the benchmarked EWI and the benchmarked MCI. Also here the EWI appears to be a very good proxy of the GOP. As before the MCI does not come close enough to the GOP to be acceptable as a good proxy.

# 7 Multi-currency Minimal Market Model

Let us now consider the stylized multi-currency minimal market model (MMM) similar to the version of the MMM described in Platen (2001) and Platen & Heath (2006). This time we model the $j$th benchmarked primary security account by the expression

$$\hat{S}_t^j = \frac{1}{Y_t^j \alpha_t^j}, \tag{7.1}$$

where $\alpha_t^j = \alpha_0^j \exp\{\eta^j t\}$, $j \in \{0, 1, \ldots, d\}$. Here $\eta^j$ is the $j$th net growth rate for $j \in \{0, 1, \ldots, d\}$, and $Y_t^j$ is the time $t$ value of the square root process $Y^j$, which

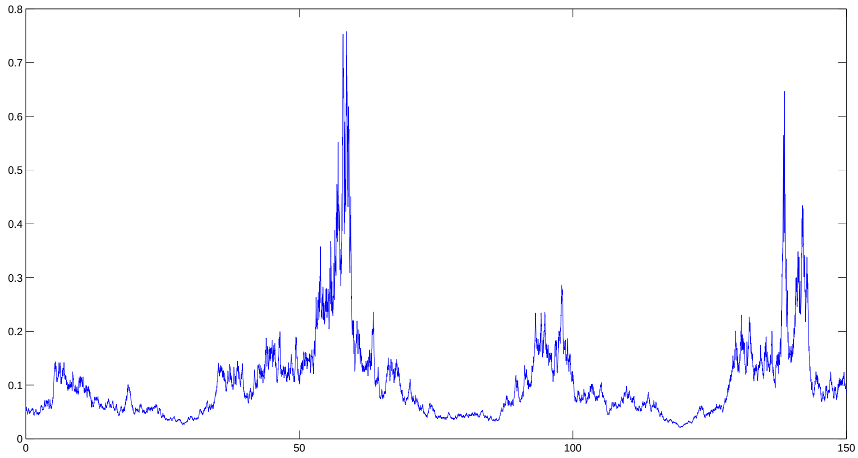


Figure 7.2: Simulated squared volatility under the MMM

satisfies the SDE

$$dY_t^j = \left(1 - \eta^j Y_t^j\right) dt + \sqrt{Y_t^j} d\tilde{W}_t^j \tag{7.2}$$

for $t \in [0, \infty)$, where we set $Y_0^j = \frac{1}{\eta^j}$ for $j \in \{0, 1, \ldots, d\}$. Here $\tilde{\boldsymbol{W}} = \{\tilde{\boldsymbol{W}}_t = (\tilde{W}_t^1, \tilde{W}_t^2, \ldots, \tilde{W}_t^d)^\top, t \in [0, \infty)\}$ is a vector of correlated Wiener processes.

Note also that under the MMM, $S^j(\varphi^j(t)) = Y_t^j \alpha_t^j$ is a squared Bessel process of dimension four in the, so called, $\varphi^j$-time. That is,

$$dS^j(\varphi^j(t)) = 4d\varphi^j(t) + 2\sqrt{S^j(\varphi^j(t))} d\bar{W}^j(\varphi^j(t)) \tag{7.3}$$

for $t \in [0, \infty)$, where one has

$$\varphi^j(t) = \frac{\alpha_0^j}{4\eta^j} \left(\exp\{\eta^j t\} - 1\right) \tag{7.4}$$

and

$$d\bar{W}^j(\varphi^j(t)) = d\tilde{W}_t^j \sqrt{\frac{d\varphi^j(t)}{dt}}. \tag{7.5}$$

The inverse $\hat{S}^j(\varphi^j(t))$ of the $j$th squared Bessel process of dimension four in $\varphi^j$-time is here represented by the following SDE

$$d\hat{S}^j(\varphi^j(t)) = -2\left(\hat{S}^j(\varphi^j(t))\right)^{\frac{3}{2}} d\bar{W}^j(\varphi^j(t)) \tag{7.6}$$

for $t \in [0, \infty)$. It can be shown that $\hat{S}^j$ is a strict supermartingale, see Protter (2004) and Platen & Heath (2006).

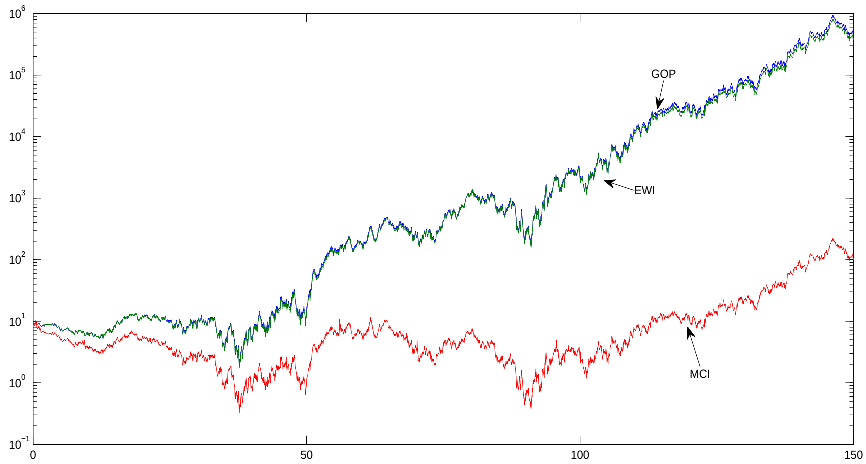


Figure 7.3: Simulated GOP, EWI and MCI under the MMM model in the log-scale

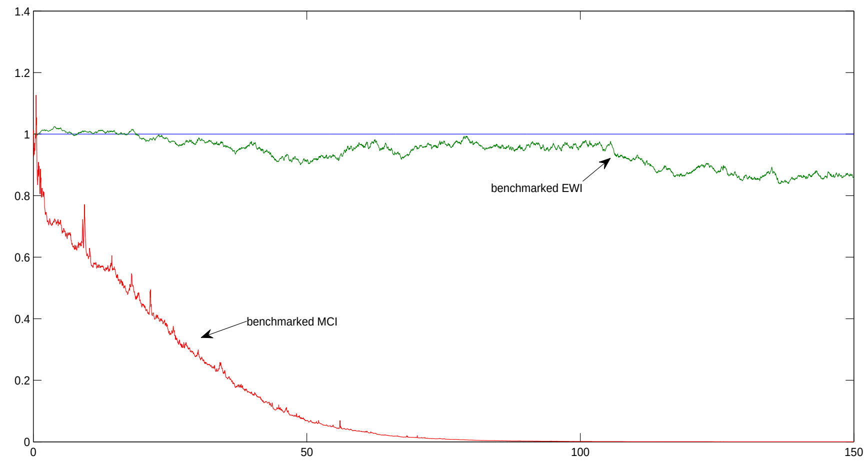


Figure 7.4: Simulated benchmarked GOP, EWI and MCI under the MMM model

Let us now explain the simulation of independent benchmarked primary security accounts under the MMM. Given the time discretization $0 < t_0 < t_1 < \dots$, where $t_i = \Delta i$, $i \in \{0, 1, \dots\}$ we first obtain (7.4) for $i \in \{0, 1, \dots\}$ and $j \in \{0, 1, \dots, d\}$.

The next step is to simulate for the $j$th benchmarked primary security account four independent Wiener processes $\bar{W}^{k,j}$, $k \in \{1, 2, 3, 4\}$ in $\varphi^j$ time. This can be achieved by simply calculating

$$\bar{W}^{k,j}_{t_{i+1}} = \bar{W}^{k,j}_{t_i} + \sqrt{\varphi^j(t_{i+1}) - \varphi^j(t_i)} Z^k_{i+1}, \tag{7.7}$$

where $Z^k_{i+1} \sim \mathcal{N}(0,1)$ is a standard Gaussian random variable. Here $k \in \{1,2,3,4\}$, $j \in \{0,1,\dots,d\}$ and $i \in \{0,1,\dots\}$.

Then the $j$th benchmarked primary security account at time $t_{i+1}$ is simulated by the expression

$$\hat{S}^j_{t_{i+1}} = \hat{S}^j\left(\varphi^j(t_{i+1})\right) = \frac{1}{\sum_{k=1}^4 \left(w^k + \bar{W}^{k,j}_{t_{i+1}}\right)^2}, \tag{7.8}$$

where $\hat{S}^j_0 = \sum_{k=1}^4 (w^k)^2$ and $i \in \{0,1,\dots\}$.

Let us now simulate the benchmarked risky primary security accounts according to the MMM. These processes are strict supermartingales. In our simulation we use the net growth rate $\eta^j = 0.09$ and scaling $\alpha^j_0 = 0.05$ for the MMM and plot in Fig. 7.1 the first 20 resulting risky benchmarked primary security accounts. The $j$th volatility equals under the MMM at time $t_i$ the expression $\hat{S}^j_{t_i}\alpha^j_{t_i}$. In Fig. 7.2 we plot a typical squared volatility under the MMM.

The GOP, EWI and MCI are displayed in Fig 7.3 in log-scale to see the significant growth over the time period. The benchmarked GOP, benchmarked EWI and benchmarked MCI are shown in Fig. 7.4. The EWI represents a good proxy for the GOP even though the benchmarked primary security accounts are here strict supermartingales and trend systematically downward, as exhibited in Fig. 7.1. The MCI again does not perform as good as the EWI and the GOP.

# 8 Multi-currency Generalized Minimal Market Model (GMMM)

Let us now describe a generalized version of the MMM, which uses some stochastic market activity time $\tau_j$. We model the $j$th benchmarked primary security account by the expression

$$\hat{S}^j_t = \frac{1}{Y^j(\tau_j(t))\alpha^j(\tau_j(t))}, \tag{8.9}$$

where $\alpha^j(\tau_j(t)) = \alpha^j_0 \exp\{\eta^j \tau_j(t)\}$ and

$$dY^j(\tau_j(t)) = \left(1 - \eta^j Y^j(\tau_j(t))\right) d\tau_j(t) + \sqrt{Y^j(\tau_j(t))}\, d\tilde{W}^j(\tau_j(t)) \tag{8.10}$$

is the SDE of a time transformed square root process, $j \in \{0,1,\dots,d\}$. Here $\tilde{\boldsymbol{W}} = \{\tilde{\boldsymbol{W}}(\tau_j(t)) = (\tilde{W}^1(\tau_j(t)), \tilde{W}^2(\tau_j(t)), \dots, \tilde{W}^d(\tau_j(t)))^\top, t \in [0,\infty)\}$ is a vector of correlated Wiener processes in $\tau_j$-time. Moreover, we use the $j$th market activity time

$$\tau_j(t) = \tau_j(0) + \int_0^t m^j_s ds, \tag{8.11}$$

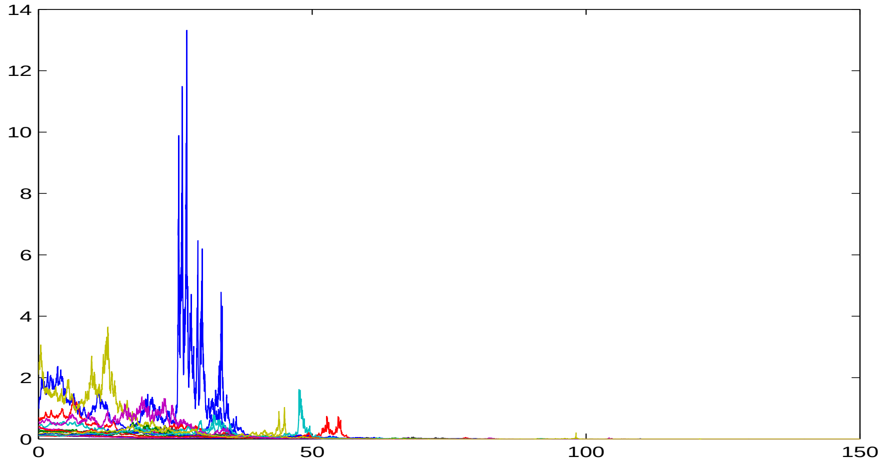


Figure 8.5: Simulated benchmarked primary security accounts under the GMMM model

where $\tau_j(0) > 0$, see Breymann, Kelly & Platen (2005). Here the $j$th market activity process $m^j$ is modeled by a linear diffusion process with SDE

$$dm_t^j = \kappa_j \left(\bar{m}_j - m_t^j\right) dt + \gamma_j m_t^j d\hat{W}_t^j, \tag{8.12}$$

for $t \in [0, \infty)$. Here the $\hat{W}^j$ are correlated Wiener processes in $t$-time. Note that the equation (8.10) can be rewritten for $Y_t^j$ in $t$-time in the following way

$$dY_t^j = \left(1 - \eta^j Y_t^j\right)\right) m_t^j dt + \sqrt{Y_t^j m_t^j} d\bar{W}_t^j, \tag{8.13}$$

for $t \in [0, \infty)$, where

$$d\bar{W}_t^j = \sqrt{\frac{1}{m_t^j}} d\tilde{W}^j(\tau_j(t)), \tag{8.14}$$

$j \in \{1, 2, \ldots, d\}$.

Since under the GMMM the $\tau_j$-time is stochastic there will be a need for numerical integration and the simulation method of the GMMM will be only almost exact. It can be, however, as accurate as required by making the time step size sufficiently small.

Given the time discretization $0 < t_0 < t_1 < \ldots$, where $t_i = \Delta i$, $i \in \{0, 1, \ldots\}$, we

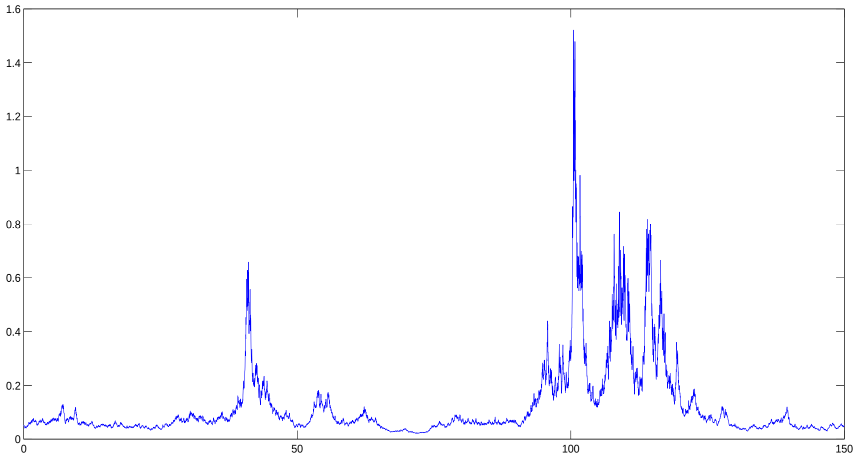


Figure 8.6: Simulated squared volatility under the GMMM

first obtain the approximate $j$th market activity

$$
\begin{aligned}
m^{j\Delta}_{t_{i+1}} &= \exp\left\{\left(-\kappa_j - \frac{1}{2}\gamma_j^2\right) t_{i+1} + \gamma_j \hat{W}^j_{t_{i+1}}\right\} \\
&\quad \times \left( m^j_{t_0} + \kappa_j \bar{m}_j \frac{\Delta}{2} \sum_{k=0}^{i} \left[ \exp\left\{\left(\kappa_j + \frac{1}{2}\gamma_j^2\right) t_k - \gamma_j \hat{W}^j_{t_k}\right\} \right.\right. \\
&\quad \left.\left. + \exp\left\{\left(\kappa_j + \frac{1}{2}\gamma_j^2\right) t_{k+1} - \gamma_j \hat{W}^j_{t_{k+1}}\right\} \right] \right)
\end{aligned}
\tag{8.15}
$$

for $t_i = \Delta i, i \in \{0, 1, \dots\}$.

Let us now introduce the $\bar{\varphi}^j$ time by the formula

$$
\bar{\varphi}^j(t_i) = \varphi^j(\tau_j(t_i)) = \frac{\alpha_0^j}{4\eta^j} \left( \exp\{\eta^j \tau_j(t_i)\} - 1 \right), \tag{8.16}
$$

for $i \in \{0, 1, \dots\}$ and $j \in \{0, 1, \dots, d\}$. Here we use the trapezoidal rule to approximate the $\tau^j$-time in the form

$$
\tau_j(t_i) \approx \tau_j(0) + \frac{\Delta}{2} \sum_{k=1}^{i} \left( m^{j\Delta}_{t_{k-1}} + m^{j\Delta}_{t_k} \right) \tag{8.17}
$$

for $i \in \{0, 1, \dots\}$, $j \in \{0, 1, \dots, d\}$.

Once the $\bar{\varphi}^j$-times are generated the simulation of the $j$th benchmarked primary security accounts under the GMMM follows the same method as described above for the MMM but now in the $\bar{\varphi}^j$ time.

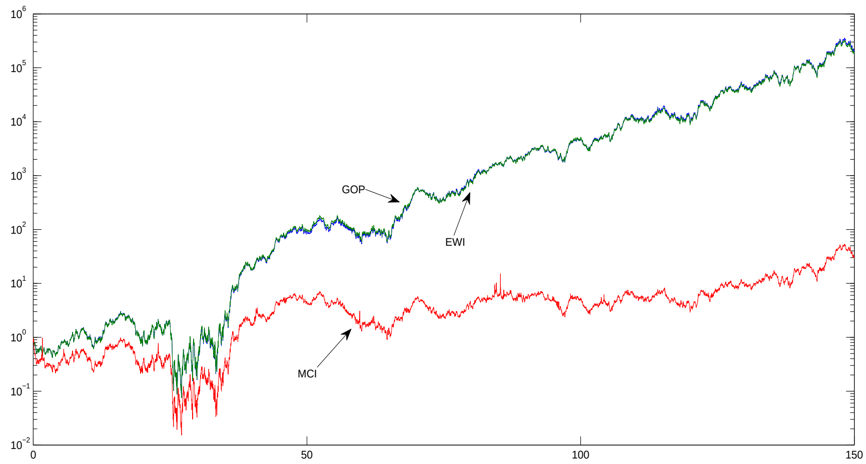


Figure 8.7: Simulated GOP, EWI and MCI under the GMMM model in the log-scale

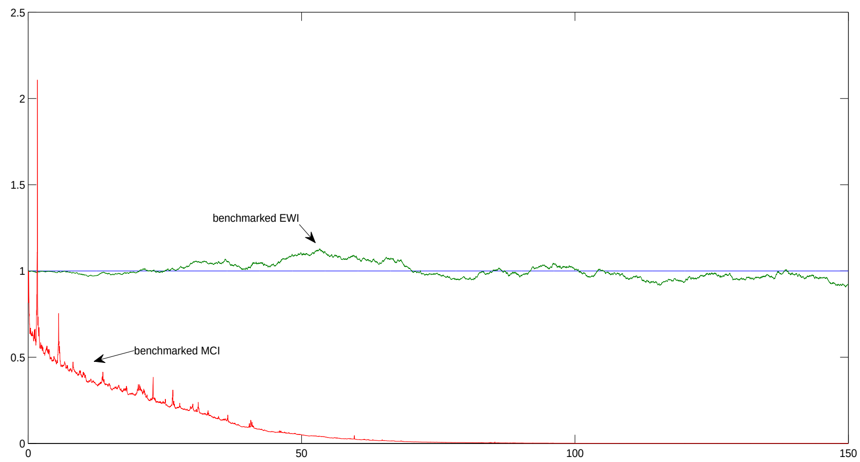


Figure 8.8: Simulated benchmarked GOP, EWI and MCI under the GMMM model

As a final model we simulate the multi-currency GMMM. This model generalizes the MMM by introducing a random market activity time $\tau_j$. In our simulation we use one common market time $\tau$ defined by the process $m$ with parameters $\bar{m} = 1$, $\kappa = 0.1$ and $\gamma = 0.1$. The net growth rate $\eta^j$ and the scaling $\alpha_0^j$ are as in the MMM. In Fig. 8.5 we illustrate the resulting benchmarked risky primary security accounts. Under the GMMM the $j$th squared volatility equal at time $t_i$ the product $\hat{S}^j_{t_i}\alpha_0^j \exp\{\eta^j\tau_j(t_i)\}m^{j\Delta}_{t_i}$. In Fig. 8.6 a typical path of squred volatility under the GMMM is exhibited.

The GOP, EWI and MCI are displayed in Fig 8.7 in the log-scale. The benchmarked GOP, benchmarked EWI and benchmarked MCI are exhibited in Fig. 8.8. Here also the benchmarked primary security accounts are strict supermartingales and trend downwards in Fig. 8.5. This systematic downward trend, however, does not destroy the property predicted by the diversification theorem that the EWI constitutes a good proxy of the GOP when observed over a considerably long time period. The MCI again does not converge in an acceptable manner to the GOP.

The last two models demonstrated that in the case when the benchmarked primary security accounts are strict supermartingales, the EWI can significantly outperform in the long run the MCI. This is an important observation since the MMM appears to be a reasonably realistic market model.

# 9 Conclusion

We considered in this paper diversified portfolios under various financial market models. All benchmarked primary security accounts under the various multi-asset models are supermartingales. The benchmarked primary security accounts of the two versions of the multi-currency minimal market model are strict supermartingales, which means that these trend systematically downwards. This is also the case for the typical market capitalization weighted index. It turns out that well diversified portfolios, such as the equal value weighted index, approximate the growth optimal portfolio rather accurately when simulated under all considered market model dynamics. However, for the two versions where benchmarked primary security accounts are strict supermartingales the difference between equal weighted index and market capitalization weighted index is remarkable. This paper successfully illustrates the applicability and robustness of the Diversification Theorem to large markets.

# References


Artzner, P. (1997). On the numeraire portfolio. In *Mathematics of Derivative Securities*, pp. 53–58. Cambridge University Press.

Bajeux-Besnainou, I. & R. Portait (1997). The numeraire portfolio: A new perspective on financial theory. *The European Journal of Finance* **3**, 291–309.

Becherer, D. (2001). The numeraire portfolio for unbounded semimartingales. *Finance Stoch.* **5**, 327–341.

Björk, T. & B. Näslund (1998). Diversified portfolios in continuous time. *European Finance Review* **1**, 361–387.

Black, F. (1976). Studies of stock market volatility changes. *Proceedings of the American Statistical Association, Business and Economic Statistics Section*, 177–181.

Black, F. & M. Scholes (1973). The pricing of options and corporate liabilities. *J. Political Economy* **81**, 637–654.

Breymann, W., L. Kelly, & E. Platen (2005). An intraday empirical analysis of currencies. (working paper).

Broadie, M. & O. Kaya (2006). Exact simulation of stochastic volatility and other affine jump diffusion processes. *Operations Research* **54**(2), 217–231.

DeMiguel, A., L. Garlappi, & R. Uppal (2009). Optimal versus naive diversification: How inefficient is the $1/n$ portfolio strategy? *Rev. Financial Studies* **22**(5), 1915–1953.

Engle, R. F. (1982). Autoregressive conditional heteroskedasticity with estimates of the variance of U.K. inflation. *Econometrica* **50**(4), 987–1007.

Fama, E. F. & K. R. French (2003). The CAPM: Theory and evidence. CRSP Working Paper No. 550, University of Chicago, 25 pp.

Fernholz, E. R. (2002). *Stochastic Portfolio Theory*, Volume 48 of *Appl. Math.* Springer.

Föllmer, H. & M. Schweizer (1993). A microeconomic approach to diffusion models for stock prices. *Math. Finance* **3**, 1–23.

Frey, R. (1997). Derivative asset analysis in models with level-dependent and stochastic volatility. Mathematics of Finance, Part II. *CWI Quarterly* **10**(1), 1–34.

Gatheral, J. (2006). *The Volatility Surface. A Practitioner's Guide.* John Wiley & Sons, Inc.

Glasserman, P. (2004). *Monte Carlo Methods in Financial Engineering*, Volume 53 of *Appl. Math.* Springer.

Goll, T. & J. Kallsen (2003). A complete explicit solution to the log-optimal portfolio problem. *Ann. Appl. Probab.* **13**(2), 774–799.

Guan, L. K., X. Liu, & T. K. Chong (2004). Asymptotic dynamics and VaR of large diversified portfolios in a jump-diffusion market. *Quant. Finance.* **4**(2), 129–139.

Heston, S. L. (1993). A closed-form solution for options with stochastic volatility with applications to bond and currency options. *Rev. Financial Studies* **6**(2), 327–343.

Hofmann, N. & E. Platen (2000). Approximating large diversified portfolios. *Math. Finance* **10**(1), 77–88.

Karatzas, I. & S. E. Shreve (1998). *Methods of Mathematical Finance*, Volume 39 of *Appl. Math.* Springer.

Kelly, J. R. (1956). A new interpretation of information rate. *Bell Syst. Techn. J.* **35**, 917–926.

Kramkov, D. O. & W. Schachermayer (1999). The asymptotic elasticity of utility functions and optimal investment in incomplete markets. *Ann. Appl. Probab.* **9**, 904–950.

Long, J. B. (1990). The numeraire portfolio. *J. Financial Economics* **26**, 29–69.

Nelson, D. B. (1990). ARCH models as diffusion approximations. *J. Econometrics* **45**, 7–38.

Platen, E. (2001). A minimal financial market model. In *Trends in Mathematics*, pp. 293–301. Birkhäuser.

Platen, E. (2002). Arbitrage in continuous complete markets. *Adv. in Appl. Probab.* **34**(3), 540–558.

Platen, E. (2004a). A benchmark framework for risk management. In *Stochastic Processes and Applications to Mathematical Finance*, pp. 305–335. Proceedings of the Ritsumeikan Intern. Symposium: World Scientific.

Platen, E. (2004b). A class of complete benchmark models with intensity based jumps. *J. Appl. Probab.* **41**, 19–34.

Platen, E. (2005). Diversified portfolios with jumps in a benchmark framework. *Asia-Pacific Financial Markets* **11**(1), 1–22.

Platen, E. & D. Heath (2006). *A Benchmark Approach to Quantitative Finance.* Springer Finance. Springer.

Platen, E. & R. Rendek (2008). Empirical evidence on Student-$t$ log-returns of diversified world stock indices. *Journal of statistical theory and practice* **2**(2), 233–251.

Platen, E. & R. Rendek (2009). Almost exact simulation of multi-dimensional stochastic volatility models. (working paper).

Protter, P. (2004). *Stochastic Integration and Differential Equations* (2nd ed.). Springer.

Simon, H. A. (1958). The size distribution of business firms. *The American Economic Review* **48**, 607–617.

Wiggins, J. B. (1987). Option values under stochastic volatility. Theory and empirical estimates. *J. Financial Economics* **19**, 351–372.